PQ Decoupling on Grid-Forming Converter Connected to a Distribution Network

Yorgo Laba, Antoine Bruyere, Frederic Colas, Xavier Guillaud

PQ Decoupling on Grid-Forming Converter Connected to a Distribution Network

Yorgo Laba
L2EP
Centrale Lille Institute
Lille, France
yorgo.laba@centralelille.fr

Antoine Bruyère
L2EP
Centrale Lille Institute
Lille, France
antoine.bruyere@centralelille.fr

Frédéric Colas
L2EP
Arts et Métiers Institute of Technology
Lille, France
frederic.colas@ensam.eu

Xavier Guillaud
L2EP
Centrale Lille Institute
Lille, France
xavier.guillaud@centralelille.fr

***Abstract*—In recent years, several works on grid-forming converters in transmission networks have been performed. Since these high voltage grids are mainly inductive, a natural decoupling exists between active and reactive power controls. This decoupling facilitates the design and the performance of the grid-forming controllers. However, in distribution applications, it is well known that the R/X ratio of the line impedance is substantially higher, preventing the system from a natural decoupling effect. This paper proposes an original solution to decouple the control and gives an application to a low voltage connection of a grid-forming converter.**

***Index Terms*—Active Power Control, Decoupling, Distribution Grid, Grid-Forming, Virtual Inductance.**

I. Introduction

The electrical energy framework is currently being restructured to increase the share of Renewable Energy Sources (RESs) in the electrical energy mix. In this context, the power sources will be connected at all the voltage levels using Power Electronic (PE) converters for their integration on the grid [1], [2]. Since the number of PE converters increases, their role in the overall power system will be correspondingly modified: Bringing inertia, supporting the voltage, contributing to the grid strength... PE converters will be required to perform a variety of system functions. In this context, the grid-forming control seems to be a promising solution to achieve these purposes. Briefly speaking, it consists in controlling the converter as a controlled-voltage source, whereas the "conventional grid-following" converter behaves as a controlled-current source. This has numerous advantages, but it also has some drawbacks. One of them is the high sensitivity to the grid impedance, not only the modulus of this impedance but also the resistive/inductive ratio. When it comes to a Voltage Source Converter (VSC) connected to a distribution system, there are two significant distinctions compared to high voltage applications: On the one hand, the VSC's connection impedance is significantly reduced, resulting in an increase in control sensitivity. Indeed, this issue has been solved for many years using the well-known concept of virtual impedance [3]–[7]. On the other hand, the ratio R/X is gradually increased, resulting in a coupling effect between active and reactive power controls [8].

Several methods have been reported to solve the coupling issue [9]. The virtual impedance-based is one of the familiar mechanisms for decoupling [3], [10], [11]. However, it requires knowledge of the grid parameters to compensate the coupling effect. Furthermore, the high virtual inductance produces a voltage drop and some harmonic disturbances.

Another decoupling method is virtual power-based, which exploits a synchronized rotation of active and reactive power [12], [13]. A similar strategy is employed in [14] by adapting the virtual f-V frame. However, both methods shift the power model's dependency from system inductance to system impedance, which, in turn, is difficult to estimate.

The final method of decoupling is the feedforward compensation [8], [15]–[19]. In contrast to virtual frame approaches, which act on the physical measures and references, feedforward compensation acts on the physical inputs of the power system. This article introduces a dynamic decoupling based on a feedforward compensatory decoupling. It is a recent innovative solution that is feasible without the grid parameters' full estimation and necessitates only the knowledge of the ratio R/X. Generally, the order of magnitude of the R/X ratio is commonly known, whereas knowledge of R and X actual values is difficult to ascertain accurately. The dynamic decoupling was first introduced in a micro-grid context in [18] without being fully explored and described. This decoupling method was devised with a virtual impedance in [19] to adjust the grid-forming on an automotive charger. However, the updated architecture was implemented with a primary grid-forming control that does not contain any inertial effect and necessitates the grid frequency estimation in the active power control. [19] assumes strong grid conditions with an adaptive decoupling architecture that adjusts the value of the anticipated R/X ratio whenever the network nature changes. This article describes and applies a new development of dynamic decoupling on a grid-forming control that mimics the Virtual Synchronous Generator (VSG) characteristics. The rest of the article is structured as follows: Section II defines the system's characteristics under study. Afterward, Section III illustrates the concept of the invented decoupling method. Furthermore, it illustrates the necessity of a grid angle estimation in the decoupling architecture. Finally, Section IV is devoted to

perform some robustness analysis of the updated architecture in various grid situations. In addition, it provides a forcefulness analysis of the ratio estimation in the dynamic decoupling.

II. Key Issues of a Grid-Forming Converter Connected to a Distrinution Grid

Fig. 1 depicts the generic organization of a grid-forming converter as defined in [20]. This converter brings an inertial effect (H) to the grid to which it is connected. In addition, the coefficient k_p is used as a damping factor. In contrast to the conventional Virtual Synchronous Machine (VSM) that is described in [21], no estimation of the grid frequency is needed. Notably, the control cited has been designed for a high voltage application with two main characteristics: Firstly, the connection impedance $X_c = L_c w_b$ is high enough. Secondly, in case of high voltage application, the grid is primarily inductive ($\frac{R_{line}}{X_{line}} \ll 1$). Hence, the active and reactive powers are considered decoupled, meaning that: The active power is linked with the control of a difference of angle ($\psi_g = \theta_m - \theta_e$) whereas the reactive power is controlled by the difference of voltage ($V_m - E_g$) (See Fig. 2). Thus, under inductive network conditions and assuming a small transmission angle ($\sin\psi_g \approx \psi_g$), active and reactive power model takes a relatively a simple linear form:

$$P_{PCC} \approx \frac{E_g V_m}{X}\psi_g \tag{1}$$

$$Q_{PCC} \approx \frac{V_m}{X}\left(V_m - E_g\right) \tag{2}$$

Where $R = R_c + R_{line};\ X = X_c + X_{line}$.

In the case of a distribution grid, the situation is fundamentally different. Firstly, the connection impedance X_c is much smaller. Since it is impossible to compare a value in the international unit (Henry), only the comparison in per-unit is consistent. It supposes to choose the nominal power (S_n) as the base value for the power (S_b) and the nominal voltage (U_n) as the base value for the voltage (U_b). Typically, a per-unit high voltage connection inductance is around 0.15 pu, a medium voltage inductance around 0.05 pu, and a low voltage impedance less than 0.02 pu. This small value potentially induces significant sensitivity challenges in terms of control. Indeed, considering (1)-(2), the linearized model reveals that its gain is represented by a division by X. So, the weakest the value of X, the biggest is the open loop gain. Adding a virtual inductance (X_v) is a classical solution to increase the value of X, which reduces the model open loop gain. Thus, the sensitivity of the control will decrease. By neglecting the dynamic terms, the implementation of virtual inductance consists of the addition of the terms $X_v w_g i_{c_q}$ and $-X_v w_g i_{cd}$ to the references of the modulated voltage $v^*_{m_{d_0}}$ and $v^*_{m_{q_0}}$, respectively, as it is shown in Fig. 1.

Secondly, the cable resistance cannot be neglected on low voltage networks. Thus, considering the hypothesis of small angle $\sin\psi_g \approx \psi_g$, active and reactive powers can be stated as follows:

$$P_{PCC} \approx \frac{V_m}{R^2 + X^2}\left(R\left(V_m - E_g\right) + X E_g \psi_g\right) \tag{3}$$

$$Q_{PCC} \approx \frac{V_m}{R^2 + X^2}\left(-R E_g \psi_g + X\left(V_m - E_g\right)\right) \tag{4}$$

Where $Z = \sqrt{R^2 + X^2}$.

Indeed, (3) and (4) reveal a coupling due to a R/X ratio strongly different in medium and low voltage grids compared to the high voltage application. The choice of a high value of the virtual inductance to compensate the resistance value was not in the scope of this work for the following reasons:

- The virtual inductance was implemented solely for robustness, not for decoupling.
- A high virtual inductance causes a significant voltage drop beyond the allowable range.
- The knowledge of the grid parameters is necessary to compensate all the resistive effects.

In the upcoming sections, the proposed methodology aims to implement a control that leads to decoupled equations for the active and reactive power.

For the rest of the article, it is assumed that the low-level control operates correctly in the steady state. Thus, the actual average value on a switching time (T_s) of the modulated voltage vmTs is nearly equal to the reference value in the control v^*_m. Hence, the following equalities for the values and the angles can be used: $V_m = V^*_m$ and $\psi_g = \psi^*_g$.

III. Principle of Dynamic Decoupling

In Section II, (3) and (4) presented coupled active and reactive power equations. Thus, the control model exploited in the transmission network is not adapted for the studied architecture of the distribution network. As clarified previously, it is primarily due to the R/X ratio, which was formerly considered negligible in transmission applications.

The classical virtual inductance introduced in the previous section permits to reduce the coupling by decreasing the total ratio R/X. However, it is a partial decoupling since the choice of the virtual inductance is fixed, and the total resistance will always persist as an impactful factor. Consequently, a decoupling method that returns to the coupling causes and fundamentals is necessary. It has to consist of returning to a model in which P_{PCC} and Q_{PCC} are controlled solely by the angle difference and the modulated voltage, respectively.

A. Dynamic Decoupling Originality

In what follows, a description of a dynamic decoupling approach is proposed. It relies on returning to the expression of active and reactive power at the transmission level (1)-(2). In this context, P_{PCC} and Q_{PCC} can be modeled as follows:

$$P_{PCC} \approx G_{11}\psi_g + G_{12}\left(V_m - E_g\right) \tag{5}$$

$$Q_{PCC} \approx G_{21}\psi_g + G_{22}\left(V_m - E_g\right) \tag{6}$$

Where $G_{11} = \frac{V_m}{R^2+X^2}XE_g, G_{21} = \frac{-V_m}{R^2+X^2}RE_g, G_{12} = \frac{V_m}{R^2+X^2}R$, and $G_{22} = \frac{V_m}{R^2+X^2}$ (With respect to (3)-(4)).

Two stages must be done to decouple P_{PCC} and Q_{PCC}:

- To decouple P_{PCC} from the V_m, the factor G_{12} must be reduced, ideally forced to zero. Thus, a new factor

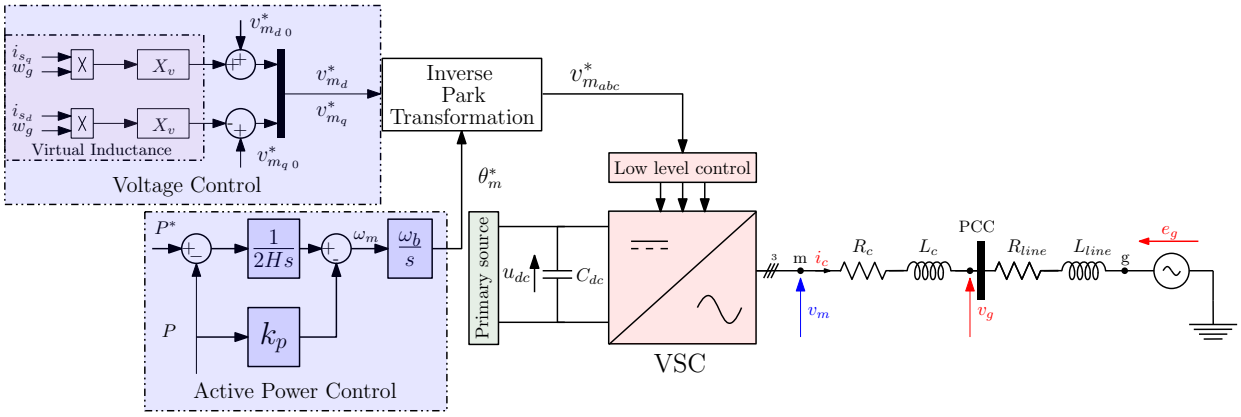

Fig. 1. Voltage Source Converter (VSC) topology in grid-connected mode.

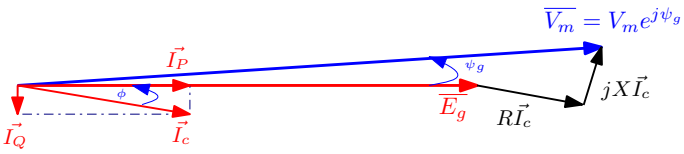

Fig. 2. Phasor diagram of the system under study.

must be added to $(V_m - E_g)$. The newly added term is: $T_{12}\,(V_m - E_g)$.

- To decouple Q_{PCC} from the ψ_g, the factor G_{21} must be reduced, ideally forced to zero. Thus, a new factor must be added to ψ_g^*. The newly added term is: $T_{21}\psi_g^*$.

After that, the new expressions of P_{PCC} and Q_{PCC} are:

$$P_{PCC} \approx (G_{11} + G_{12}T_{12})\,\psi_g^{dec} + (G_{11}T_{12} + G_{12})(V_m^{dec} - E_g) \tag{7}$$

$$Q_{PCC} \approx (G_{22} + T_{12}G_{12})(V_m^{dec} - E_g) + (G_{21} + G_{22}T_{21})\psi_g^{dec} \tag{8}$$

Where ψ_g^{dec} and V_m^{dec} are the angle difference and the voltage reference found before the added decoupling factors, respectively. To have an active power that is solely dependent on ψ_g^{dec}, the term $G_{11}T_{12} + G_{12}$ must be equal to zero. Thus:

$$T_{12} = -\frac{G_{12}}{G_{11}} = -\frac{R}{XE_g} \tag{9}$$

The same methodology goes for the reactive power:

$$T_{21} = -\frac{G_{21}}{G_{22}} = \frac{RE_g}{X} \tag{10}$$

Subsequently, following the dynamic decoupling implementation, the new expressions of P_{PCC} and Q_{PCC} are:

$$P_{PCC} \approx (G_{11} + G_{12}T_{12})\,\psi_g^{dec} = \frac{E_g V_m^{dec}}{X}\psi_g^{dec} \tag{11}$$

$$Q_{PCC} \approx (G_{22} + T_{12}G_{12})(V_m^{dec} - E_g) = \frac{V_m}{X}\left(V_m^{dec} - E_g\right) \tag{12}$$

The modified control architecture, as well as the power model, are represented in Fig. 3. As it is shown in the proposed decoupling function, only an estimation of the ratio $\frac{R}{X}$ is needed. The estimated ratio will be noted as $\left(\frac{R}{X}\right)_{es}$ for the rest of the article, as shown in Fig. 3. In addition, as it will be demonstrated in the upcoming section, the proposed decoupling is robust to any error that may occur on the $\left(\frac{R}{X}\right)_{es}$'s estimation.

As clarified in (11)-(12), the dynamic decoupling returns to the exact expressions of the transmission level given by (1) and (2), which means a decoupled formulation and a purely inductive model. Subsequently, the high resistance of the distribution network does not appear. For the remainder of the paper, the following nomenclature is used:

- "Classical grid-forming" control stated in [20], where no decoupling function is inserted due to the assumption of an inductive grid, as declared in (1)-(2) and Fig. 1.
- "Decoupled grid-forming" control, where the virtual inductance and the decoupling function advocated in this paper are added to the "classical grid-forming".

B. Dynamic Decoupling consequences

Where the grid resistance cannot be neglected, typically on low or medium voltage applications, grid-forming control architecture is modified as described on Fig. 3. Then, the two degrees of freedom of the control are the same as for conventional inductive situations: The modulated voltage angle to control the active power and the voltage magnitude to control the reactive power.

As it can be noticed in the theoretical explanations of virtual inductance and dynamic decoupling, implementing the "decoupled grid-forming" induces a voltage variation by adding other terms to V_m^*. This variation should not be ignored, and it must be guaranteed that the voltage stays within the permissible range to comply with the network grid codes [22], [23]. Since it is not in the scope of this article, the voltage shapes at the PCC are not given. However, it has been verified for all tests in this paper that the steady-state voltage is always in the 1pu ± 10 % range. The explained profits and impacts of the updated architecture will be profoundly explored in the

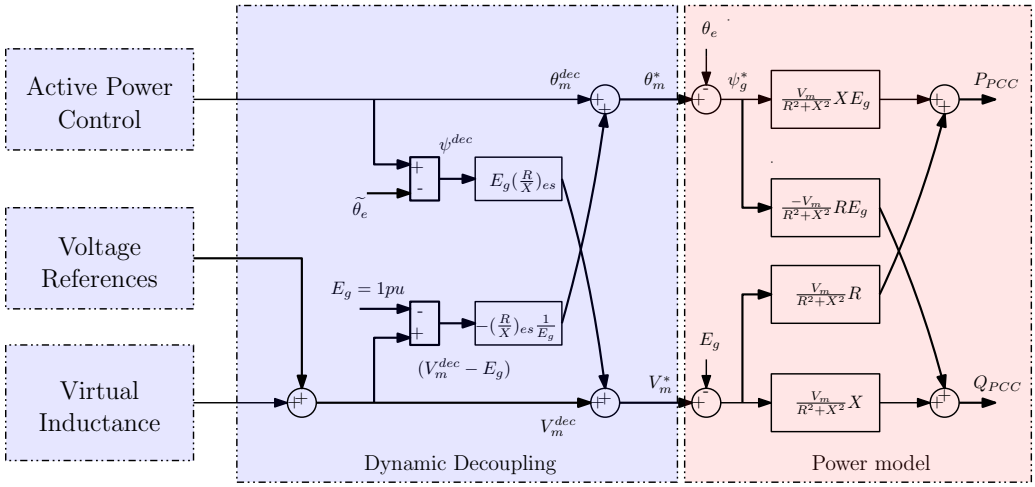

Fig. 3. Implementation of dynamic decoupling to the existing grid-forming control.

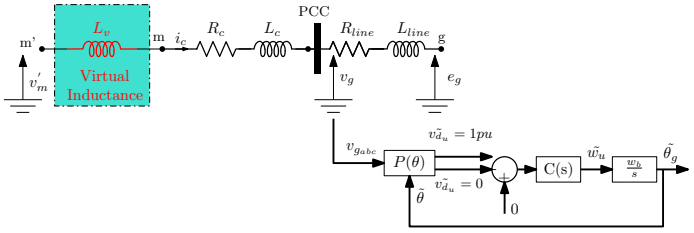

Fig. 4. PLL implementation to estimate the grid angle.

TABLE I
REFERENCE SYSTEM PARAMETERS

Symbol	Quantity	Symbol	Quantity
$P_n = S_{n3\varphi}$	22 KW	U_{ac}	400 V
R_{line}	$4.45X_{line}$	f_r	50 Hz
X_c	0.02 pu	w_b	$2\pi f_r$
R_c	0.002 pu	H	0.5 s
U_{dc}	800 V	ζ	0.7

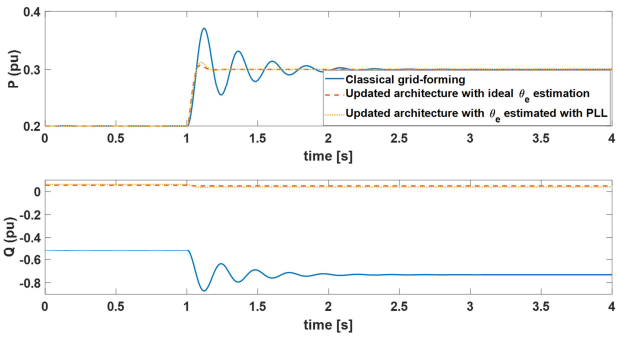

Fig. 5. Decoupled grid-forming architecture effect on system behavior.

upcoming subsection by studying the system under different circumstances of low voltage distribution networks.

C. Necessity of the Grid Angle Estimation θ_e

As seen in Fig. 3, the decoupling architecture requires having a measurement of $\Psi_g = \theta_m - \theta_e$ to perform its functionality. Indeed, the converter angle θ_m is generated by the control. However, the grid angle θ_e is not measurable and is not accessible. Therefore, an estimation of θ_e is necessary. In [19], the control architecture was carried out supposing a perfect estimation of the grid angle θ_e. Since such approach is not realistic, this paper illustrates the use of the Phased Locked Loop (PLL) to obtain a measure of θ_e. As shown in Fig. 4, the PLL calculates the grid's angle and frequency at the PCC. Therefore, the estimated angle is the one at $v_g(\theta_g)$. Since the distribution network is resistive, the grid line consumes a meager amount of reactive power. Consequently, the $\tilde{\theta_g}$ estimated by the PLL is very close to θ_e. It is noteworthy that the implementation of the PLL does not intervene in the direct control of active and reactive power. It does not reduce system stability in weak grid situations, as in the case of the grid-following control. To prove the efficacy of the proposed method, a comparative study is performed in Fig. 5. It compares the active and reactive power behavior with the classical grid-forming control, with the decoupled grid-forming accompanied by ideal θ_e estimation, and with a decoupled grid forming that employs the PLL estimation. The results considered are performed under the system and control parameters of Table I.

Fig. 5 exhibits the importance of the decoupled grid-forming compared to the classical one. First, the decoupling factor between P_{PCC} and Q_{PCC} collapses. Furthermore, the oscillations are eliminated, and the time response is adjusted. Second, the results proved the effectiveness of estimating θ_e by a PLL. Indeed, there is no noticeable difference with the case where θ_e is ideally estimated.

IV. Robustness Studies Analysis

A. Grid Impedance Variation

It was demonstrated in [19] that the dynamic decoupling operates accurately in all lines types, starting with high voltage networks ($\frac{R_{line}}{X_{line}} \approx 0.1$), and progressing to medium voltage

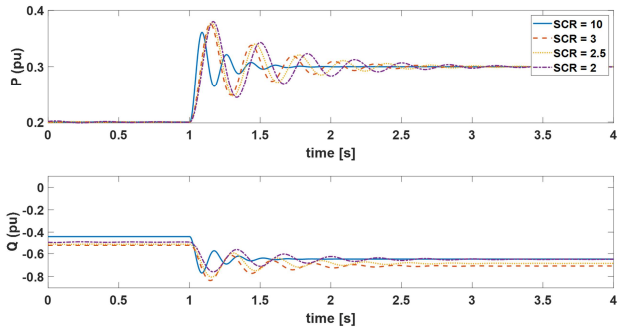

Fig. 6. SCR parametric study with the classical formulation of grid-forming.

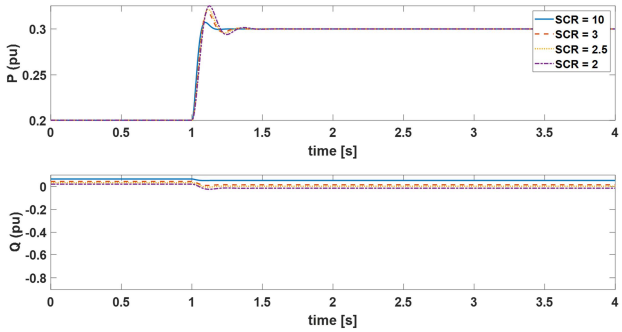

Fig. 7. SCR parametric study with the updated architecture of grid-forming.

network ($\frac{R_{line}}{X_{line}} \approx 1$), and arriving to extreme low voltage network conditions ($\frac{R_{line}}{X_{line}} \approx 7$). The study cited was performed with strong grid condition with relatively high Short Circuit Ratio (SCR). Regarding the difference in cable properties at distribution networks, many grids have significant lengths (farms in rural regions) or relatively short distances (building substations and risers). There are also old wires with low sections that must not be disregarded. Consequently, the ratio $\frac{R_{line}}{X_{line}}$ will be fixed based on low voltage cables conditions [24] (Table I) and the SCR will be gradually decreased to evaluate the suggested control architecture on weak network conditions. The simulation results are proposed to assess the enhancement brought by the decoupled grid-forming. First, Fig. 6 exhibits the parametric study before the employment of the proposed approach. Two main points can be drawn:

- Rise of a coupling effect between active and reactive power response. It is due to the distribution network's resistive nature, as shown in (3) and (4).
- Increase in the system's time response and appearance of oscillation in the transient state. It is due to the reduction in the connection inductance followed by the increase of the line resistance.

Getting to the final results of Fig. 7, the control proved its efficacy. First, the coupling is nearly null, and the remaining small coupling is not a flaw of the suggested method since it is also found on the transmission level. Furthermore, the reactive power is driven to zero due to its simplified expression. This allows reducing the power factor in order to respect the static conditions of the power electronic converter. In a nutshell, the results demonstrated the efficacy of the theoretical explanations deliberated previously.

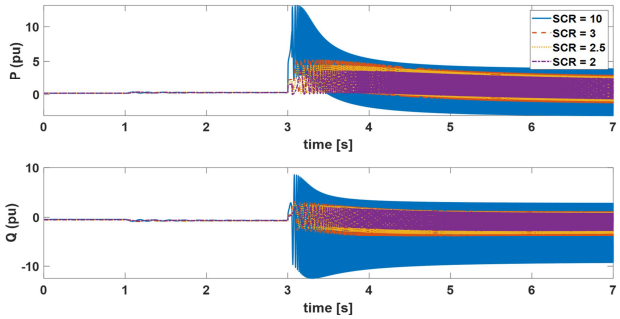

Fig. 8. SCR parametric study considering a voltage-ride through on the voltage source with the conventional architecture of grid-forming.

B. Voltage-Ride-Through

The results shown in the previous subsections revealed that the application of the conventional grid-forming illustrated in [20] leads to two main issues when a reference is applied to the active power: The rise of a high coupling factor on Q_{PCC} and the presence of oscillations in the transient state of the active power response. Under some settings, such oscillations may be considered acceptable since they occasionally have a tolerable overshoot and good time response elimination. Furthermore, because the system converges to the expected steady-state response under all situations, it may not affect its overall stability. However, the events shown in Fig. 6 and Fig. 7 represent the converter's regular operating settings. However, other abnormal occurrences, such as voltage-ride-through, may occur on the network while connecting the power converter to it. To demonstrate the significance of the suggested architecture under atypical circumstances, the same parametric study shown before will be replicated, but with a voltage-ride-through on the voltage source e_g, with an amplitude of $\Delta E_g = 0.8$ pu and duration of $\Delta t = 0.05$ s, added at t = 3 s.

As seen in Fig. 8, the presence of oscillations in normal situations has spread the instability across the system when using the classical grid-forming. However, since the decoupled grid-forming architecture has led to a more robust system, power responses restored their steady state values after a voltage-ride-through, as seen in Fig. 9.

C. Error on the R/X Estimation

Previous results reveal the advantages of dynamic decoupling in control architecture. So far, the decoupling has been performed by assuming a known value for the R/X ratio. As a result of the converter's many applications (such as the electric vehicle), it can be linked to a different network type at any moment. Thus, the decoupling architecture must update its $\left(\frac{R}{X}\right)_{es}$ at each time accordingly. In this context, Fig. 10 depicts the system behavior with various error estimations on the $\left(\frac{R}{X}\right)_{es}$ (ideally equal to 4.45). As depicted by the results, the proposed decoupling approach has a high accuracy. Even if

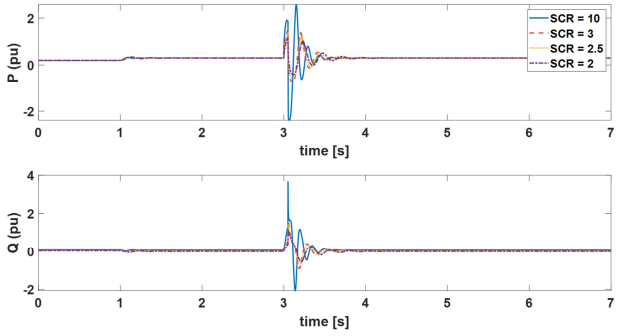

Fig. 9. SCR parametric study considering a voltage-ride-through on the voltage source with the updated architecture of grid-forming.

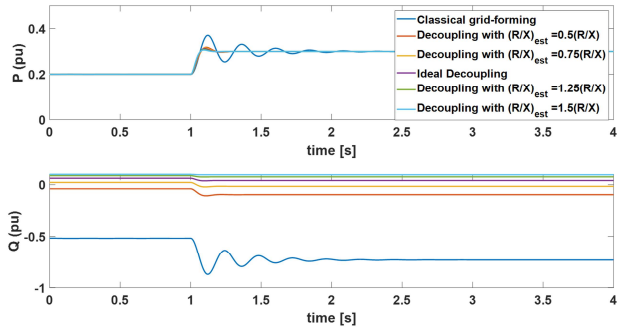

Fig. 10. Study of R Study of $\left(\frac{R}{X}\right)_{es}$'s influence estimation on the system dynamics and robustness.

the estimation of R/X is 50% off, the coupling factor remains in the same range. As a result, it is always more practical to implement the decoupling even with significant errors on the $\left(\frac{R}{X}\right)_{es}$ then not implement any form of dynamic decoupling.

V. Conclusion

Achieving a high level of controllability of the converters comprising the network at the distribution level necessitates considering several factors, including a low connection inductance and a resistive network line. The virtual inductance value has been adjusted to ensure the restoration of a higher connection inductance. The hybrid control embedding the virtual inductance and the dynamic decoupling has allowed being less susceptible to the topological changes of the grid. In addition, it allowed returning to the well-mastered reference case of the "conventional grid-forming" architecture that is defined at the transmission level for naturally inductive grids.

References

[1] ENTSO-E, "Research, Development & Innovation Roadmap 2020 – 2030", p. 33.

[2] International Energy Agency et Réseau de Transport d'Electricité, *Conditions and Requirements for the Technical Feasibility of a Power System with a High Share of Renewables in France Towards 2050*. OECD, 2021.

[3] C. Li, S. K. Chaudhary, M. Savaghebi, J. C. Vasquez, et J. M. Guerrero, "Power Flow Analysis for Low-Voltage AC and DC Microgrids Considering Droop Control and Virtual Impedance", *IEEE Trans. Smart Grid*, vol. 8, no 6, p. 2754-2764, nov. 2017.

[4] L. Huang, C. Wu, D. Zhou, et F. Blaabjerg, "Impact of Virtual Admittance on Small-Signal Stability of Grid-Forming Inverters", in *2021 6th IEEE Workshop on the Electronic Grid (eGRID)*, New Orleans, LA, USA, nov. 2021, p. 1-8.

[5] B. Wei, A. Marzabal, R. Ruiz, J. M. Guerrero, et J. C. Vasquez, "DAVIC: A New Distributed Adaptive Virtual Impedance Control for Parallel-Connected Voltage Source Inverters in Modular UPS System", *IEEE Trans. Power Electron.*, vol. 34, no 6, p. 5953-5968, juin 2019.

[6] J. He et Y. W. Li, "Analysis, Design, and Implementation of Virtual Impedance for Power Electronics Interfaced Distributed Generation", *IEEE Trans. Ind. Appl.*, vol. 47, no 6, p. 2525-2538, nov. 2011.

[7] B. Rathore, S. Chakrabarti, et L. Srivastava, "A Self-Regulated Virtual Impedance control of VSG in a microgrid", *Electr. Power Syst. Res.*, vol. 197, p. 107289, août 2021.

[8] M. Li, Y. Wang, Y. Liu, N. Xu, S. Shu, et W. Lei, "Enhanced Power Decoupling Strategy for Virtual Synchronous Generator", *IEEE Access*, vol. 8, p. 73601-73613, 2020.

[9] A. Bidram et A. Davoudi, "Hierarchical Structure of Microgrids Control System", *IEEE Trans. Smart Grid*, vol. 3, no 4, p. 1963-1976, déc. 2012.

[10] H. Zhang, S. Kim, Q. Sun, et J. Zhou, "Distributed Adaptive Virtual Impedance Control for Accurate Reactive Power Sharing Based on Consensus Control in Microgrids", *IEEE Trans. Smart Grid*, vol. 8, no 4, p. 1749-1761, juill. 2017.

[11] P. C. Nakka et M. K. Mishra, "Droop characteristics based damping and inertia emulation of DC link in a hybrid microgrid", *IET Renew. Power Gener.*, vol. 14, no 6, p. 1044-1052, avr. 2020.

[12] K. De Brabandere, B. Bolsens, J. Van den Keybus, A. Woyte, J. Driesen, et R. Belmans, "A Voltage and Frequency Droop Control Method for Parallel Inverters", *IEEE Trans. Power Electron.*, vol. 22, no 4, p. 1107-1115, juill. 2007.

[13] T. Wu, Z. Liu, J. Liu, S. Wang, et Z. You, "A Unified Virtual Power Decoupling Method for Droop-Controlled Parallel Inverters in Microgrids", *IEEE Trans. Power Electron.*, vol. 31, no 8, p. 5587-5603, août 2016.

[14] Y. Li et Y. W. Li, "Power Management of Inverter Interfaced Autonomous Microgrid Based on Virtual Frequency-Voltage Frame", *IEEE Trans. Smart Grid*, vol. 2, no 1, p. 30-40, mars 2011.

[15] J.-Y. Park, J. Ban, Y.-J. Kim, et X. Lu, "Supplementary Feedforward Control of DGs in a Reconfigurable Microgrid for Load Restoration", *IEEE Trans. Smart Grid*, vol. 12, no 6, p. 4641-4654, nov. 2021.

[16] T. Wen, X. Zou, X. Guo, D. Zhu, L. Peng, et X. Wang, "Feedforward Compensation Control for Virtual Synchronous Generator to Improve Power Decoupling Capability", in *2019 14th IEEE Conference on Industrial Electronics and Applications (ICIEA)*, Xi'an, China, juin 2019, p. 2528-2533.

[17] Z. Peng et al., "Droop Control Strategy Incorporating Coupling Compensation and Virtual Impedance for Microgrid Application", *IEEE Trans. Energy Convers.*, p. 1-1, 2019.

[18] Xiangwu Yan et Ye Zhang, "Power coupling analysis of inverters based on relative gain method and decoupling control based on feedforward compensation", in *International Conference on Renewable Power Generation (RPG 2015)*, Beijing, China, 2015, p. 5 .-5.

[19] Y. Laba, A. Bruyere, F. Colas, X. Guillaud, et B. Silvestre, "Operating Grid-Forming Control on Automotive Reversible Battery Charger", in *2021 IEEE Vehicle Power and Propulsion Conference (VPPC)*, Gijon, Spain, oct. 2021, p. 1-6.

[20] T. Qoria, E. Rokrok, A. Bruyere, B. Francois, et X. Guillaud, "A PLL-Free Grid-Forming Control With Decoupled Functionalities for High-Power Transmission System Applications", *IEEE Access*, vol. 8, p. 197363-197378, 2020.

[21] S. D'Arco et J. A. Suul, "Equivalence of Virtual Synchronous Machines and Frequency-Droops for Converter-Based MicroGrids", *IEEE Trans. Smart Grid*, vol. 5, no 1, p. 394-395, janv. 2014.

[22] The European Commission, "COMMISSION REGULATION (EU) 2016/ 631 - of 14 April 2016 - establishing a network code on requirements for grid connection of generators", *Official Journal of the European Union*, Apr. 2016. p. 68.

[23] EN 5054-1, "Requirements for generating plants to be connected in parallel with distribution networks - Part 1: connection to a LV distribution network - Generating plants up to and including Type B", p. 68.

[24] Nexans Olex New Zealand, "Power Cable Catalogue" 2012 Edition.